# Activity Coefficients at Infinite Dilution of Organic Solutes in the Ionic Liquid 1-Ethyl-3-methyl-imidazolium Nitrate

**Marek Sobota, Vladimír Dohnal,* and Pavel Vrbka**

*Department of Physical Chemistry, Institute of Chemical Technology, 166 28 Prague 6, Czech Republic*

*Received: December 15, 2008; Revised Manuscript Received: January 23, 2009*

Infinite dilution activity coefficients $\gamma_1^\infty$ and gas−liquid partition coefficients $K_L$ of 30 selected hydrocarbons, alcohols, ketones, ethers, esters, haloalkanes, nitrogen- and sulfur-containing compounds in the ionic liquid (IL) 1-ethyl-3-methylimidazolium nitrate [EMIM][$NO_3$] were determined by gas−liquid chromatography at five temperatures in the range from 318.15 to 353.15 K. Relative contribution of adsorption at gas−liquid interphase to the overall solute retention, as examined by varying sample size and IL loading in the column, was found negligible. Partial molar excess enthalpies and entropies at infinite dilution were derived from the temperature dependence of the $\gamma_1^\infty$ values. The linear free energy relationship (LFER) solvation model was used to correlate successfully the $K_L$ values. The LFER correlation parameters and excess thermodynamic functions were analyzed to disclose molecular interactions operating between the IL and the individual solutes. In addition, the promising potential of [EMIM][$NO_3$] for applications in solvent-aided separation processes was identified, the selectivities of [EMIM][$NO_3$] for separation of aromatic hydrocarbons and thiophene from saturated hydrocarbons ranking among the highest ever observed with ILs or molecular solvents.

## Introduction

Ionic liquids (ILs) are defined as molten salts with a melting point temperature below 100 °C. In recent years, these novel materials have been increasingly gaining a massive interest of researchers because of technologically attractive properties, such as negligible vapor pressure, low flammability, high solubility of organic, inorganic, and polymeric substances, low corrosion tendencies, and good thermal stability.[1] ILs can offer economically and environmentally more favorable alternatives to common organic solvents, for example, in transition metal and enzymatic catalytic reactions and separations of organic substances by means of extraction or extractive distillation. In this respect, ILs are often regarded as *green* solvents. The above-mentioned and many other possible applications of ILs have been described in the literature.[2−7]

Because of the vast number of possible anion and cation combinations, ILs with very different physicochemical properties can be prepared, which opens prospects for tailoring them for specific applications in particular processes. Obviously, for exploration and design of such applications, knowledge of interactions of process components with ILs is needed. A suitable and widely accepted approach for the description of interactions of organic solutes (1) with ILs as solvents (2) is the experimental determination of limiting activity coefficients at infinite dilution $\gamma_1^\infty$. The infinite dilution activity coefficient is a fundamental thermodynamic quantity providing a convenient measure of solution nonideality and component compatibility. Classical gas−liquid chromatography (GLC) has been proven to be a good tool for the determination of $\gamma_1^\infty$ values of volatile organic compounds (VOC) in nonvolatile ILs by a number of researchers.[8−14] In the GLC method the retention of VOC in a column with IL as a stationary phase is measured.

The aim of this work was to examine interactions of selected VOCs with the ionic liquid 1-ethyl-3-methylimidazolium nitrate [EMIM][$NO_3$].

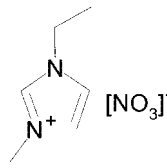


This imidazolium-based IL was chosen for several reasons. First, [EMIM][$NO_3$] belongs to the group of small polar ILs which seem to show high selectivity for separation of aliphatic and aromatic hydrocarbons, but no experimental data on $\gamma_1^\infty$ in this IL have been reported so far. Second, because of its relatively small ions, this IL exhibits an extremely strong cohesion,[15] yet its melting point temperature is sufficiently low (40 °C). Considering the chemical structure of the IL, its capability for various types of specific interactions can be anticipated which adds to the expectation of its separation selectivity. Last but not least, [EMIM][$NO_3$] is commercially available in high purity (>99%) and, as an IL of the third generation, does not contain halogens.

In this paper GLC measurements of the infinite dilution activity coefficients $\gamma_1^\infty$ and gas−liquid partition coefficients $K_L$ of 30 selected hydrocarbons, alcohols, ketones, ethers, esters, haloalkanes, and nitrogen- or sulfur-containing compounds in [EMIM][$NO_3$] as a function of temperature are presented. The obtained thermodynamic properties are analyzed to disclose the underlying intermolecular interactions governing the observed behavior and to identify the potential of [EMIM][$NO_3$] to be utilized as an entrainer in solvent-aided separations.

## Theory

In gas−liquid chromatography (GLC), the infinite dilution activity coefficient $\gamma_1^\infty$ and the gas−liquid partition coefficient

* To whom correspondence should be addressed. E-mail: dohnalv@vscht.cz. Tel.: +420 220 444 297. Fax: +420 220 444 333. Address: Department of Physical Chemistry, Institute of Chemical Technology, Technická 5, 166 28 Prague 6, Czech Republic.

10.1021/jp811041k CCC: $40.75 
Published on Web 03/02/2009

$K_L = (c_1^L/c_1^G)$ for a solute (1) partitioning between a carrier gas (2) and a nonvolatile liquid solvent (3) are calculated from the solute retention according to the following equations[16]

$$\ln \gamma_1^\infty = \ln\left(\frac{RTm_3}{V_N p_1^s M_3}\right) - \left[\frac{(B_{11} - v_1^L)p_1^s}{RT}\right] + \left[\frac{(2B_{12} - \bar{v}_1^\infty)J_3^4 p_0}{RT}\right] \quad (1)$$

$$\ln K_L = \ln\left(\frac{V_N \rho_3}{m_3}\right) + \left[\frac{(2B_{12} - \bar{v}_1^\infty)J_3^4 p_0}{RT}\right] \quad (2)$$

where $T$ is temperature of the column, $m_3$, $M_3$, and $\rho_3$ are the mass, molar mass, and density of the solvent, respectively, and $p_1^s$ is the saturated vapor pressure of the solute. The first term on the right-hand side of eq 1 and eq 2 is of the principal importance for the calculation of $\gamma_1^\infty$ and $K_L$, respectively, while the remaining terms represent relatively small corrections for gas-phase nonideality. In these corrective terms $B_{11}$ stands for the second virial coefficient of the pure solute, $B_{12}$ for the second cross virial coefficient for the solute-carrier gas interaction, $v_1^L$ for molar volume of the pure liquid solute, $\bar{v}_1^\infty$ for partial molar volume of the solute at infinite dilution in component 3, and $p_0$ for the column outlet pressure. The net retention volume $V_N$ is calculated from the following equation

$$V_N = J_3^2 F(t_R - t_D) \quad (3)$$

where $t_R$ is the retention time of a given solute, $t_D$ is the retention time of the nonretainable component, and $F$ is the carrier gas flow at the column temperature and column outlet pressure. The corrections $J_n^m$ used in eqs 1−3 account for compressibility of the mobile phase and are defined as[16]

$$J_n^m = \frac{n}{m}\left[\frac{(p_i/p_0)^m - 1}{(p_i/p_0)^n - 1}\right] \quad (4)$$

where $p_i$ stands for the column inlet pressure.

If the infinite dilution activity coefficient is determined as a function of temperature, $\ln \gamma_1^\infty$ can be split to its respective enthalpy and entropy components

$$\ln \gamma_1^\infty = \frac{\bar{H}_1^{E,\infty}}{RT} - \frac{\bar{S}_1^{E,\infty}}{R} \quad (5)$$

Assuming that the temperature dependence follows a linear van't Hoff plot

$$\ln \gamma_1^\infty = a/T + b \quad (6)$$

the partial molar excess enthalpy $\bar{H}_1^{E,\infty} = Ra$ and entropy $\bar{S}_1^{E,\infty} = -Rb$ at infinite dilution can be obtained from its slope and intercept, respectively.

## Experimental Details

**Materials.** The ionic liquid 1-ethyl-3-methylimidazolium nitrate ([EMIM][$NO_3$], $M = 173.17$ g/mol) produced by Fluka was supplied by Sigma-Aldrich. Its purity according to the producer's specification was >99%, certified water content being ≤0.2% (mass basis). Because of its hygroscopicity, the IL was handled with special precautions to avoid any contact with moisture (see below). The IL samples contained in the GLC columns used for retention measurements underwent efficient drying in situ during the column conditioning. As determined by ad hoc experiments, the residual water contents (Karl Fischer titration) of these samples were below 300 ppm (mass basis).

The volatile organic compounds (VOC) used as solutes were all of p.a. purity grade. The solute purity, however, need not be regarded as critical for the $\gamma_1^\infty$ determinations. As gas chromatography itself is a separation method it can be well assumed that any solute impurities that would possibly affect the measured retention are separated in the course of the chromatographic process. Therefore all solutes were used without further purification.

Inerton Super (Lachema, Czech Republic) of (0.125−0.160) mm granularity was used as a solid support for IL in the GLC column. This high-quality, AW-DMCS diatomaceous solid support is characterized by an extreme adsorption and catalytic inertness and a very low specific surface area ((0.3−0.55) $m^2/g$).[17]

Dichloromethane (Penta, Czech Rep.) used as a solvent in the coating process was of p.a. purity grade, the certified water content being ≤0.02% (mass basis). It was dried with molecular sieves prior to use to decrease further its water content.

**Apparatus.** The measurements were performed on a computer controlled model 6890 Plus Agilent gas chromatograph (Agilent Technologies, USA) equipped with a flame ionization detector (FID). Stainless steel packed columns with outer diameter of $^1/_4$ in (wall thickness 1 mm) and two lengths of 1.2 and 1.7 m were used. Solute samples were injected by a 7683 series Agilent autoinjector. Nitrogen served as the carrier gas. The signal from the detector was recorded and processed by a PC with the ChemStation software (Agilent Technologies, USA). A Varian (model Cary 50Bio) UV spectrophotometer was used in the determination of the IL loading of the support.

**Column Preparation.** All manipulations during the column preparation (including weighing) were performed in a spacious glovebox under dry air atmosphere. As an initial step, the solid support was loaded with the desired amount of IL. In this work, the IL loading $\lambda$ of the support varied from 0.11 to 0.15. The IL average film thickness $d_f$ from 0.2 to 0.3 $\mu$m corresponding to such values of $\lambda$ and to the support used is well within the range of the $d_f$ values corresponding to GLC $\gamma_1^\infty$ measurements reported in the recent literature. In the coating process, the support material was dispersed in a solution of the IL in dichloromethane and the volatile solvent from the slurry was then slowly evaporated using a rotary vacuum evaporator. Prolonged drying of the coated material in the evaporator for several additional hours ensured complete removal of the dichloromethane.

The column was carefully packed with the coated support through a funnel attached at the inlet while applying reduced pressure exerted by a membrane pump at the outlet. The mass of the coated support charged in the column was obtained alternatively from differential weighing of the material or the column. Since both values were generally in very good agreement (difference <0.1% of total support packed), deter-

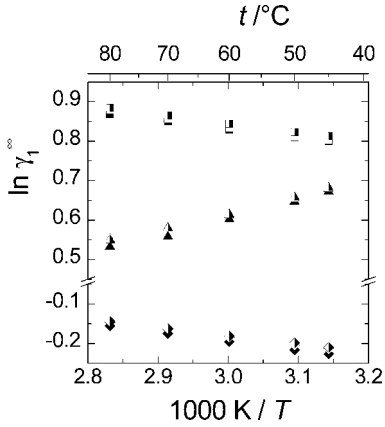


**Figure 1.** Comparison of $\gamma_1^\infty$ values obtained from measurements on three columns loaded with different amounts of [EMIM][$NO_3$] for solutes exhibiting sufficient retention: ◆, acetonitrile, 1.194 g of IL; ◇, acetonitrile, 1.413 g of IL; half-filled diamond, acetonitrile, 2.064 g of IL; ▲, propan-2-ol, 1.194 g of IL; △, propan-2-ol, 1.413 g of IL; ◭, propan-2-ol, 2.064 g of IL; ■, acetone, 1.194 g of IL; □, acetone, 1.413 g of IL; ◨, acetone, 2.064 g of IL.

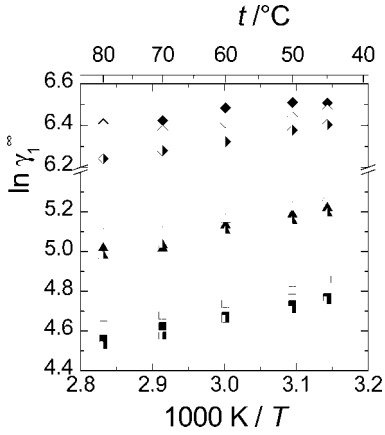


**Figure 2.** Comparison of $\gamma_1^\infty$ values obtained from measurements on three columns loaded with different amounts of [EMIM][$NO_3$] for solutes exhibiting weak retention: ◆, octane, 1.194 g of IL; ◇, octane, 1.413 g of IL; half-filled diamond, octane, 2.064 g IL; ▲, methylcyclohexane, 1.194 g IL; △, methylcyclohexane, 1.413 g IL; ◭, methylcyclohexane, 2.064 g of IL; ■, cyclohexane, 1.194 g of IL; □, cyclohexane, 1.413 g of IL; ◨, cyclohexane, 2.064 g of IL.

mination of the mass of the support in the column can be considered accurate.

**Determination of the IL Loading.** Two distinct procedures, gravimetric and spectrophotometric, were used to determine the IL loading $\lambda$ of the solid support. An aliquot (approximately 2 g) of coated support was accurately weighed and the IL was extracted with several portions of dichloromethane through a preweighed fritted glass funnel into a preweighed graduated flask. The support was dried and weighed. Dichloromethane in the extract was slowly evaporated in the nitrogen atmosphere and the graduated flask was weighed afterward. The mass of the IL in the sample was obtained as (i) the weight drop of the coated support upon extraction and (ii) by weighing the IL in the extract.

For the spectrophotometric determination, the extracted IL in the graduated flask was subsequently dissolved in water. The aqueous solution was further diluted to match the appropriate absorbance level. The exact concentration of [EMIM][$NO_3$] in the diluted aqueous solution was determined by measuring its absorbance at 203 nm (a saddle in the absorbance−wavelength dependence) and comparing it with the calibration line determined in parallel. The calibration line was based on absorbance measurements for six standard IL solutions. The calibration results were found to obey closely an absorbance−concentration proportionality implied by the Lambert−Beer law. At least two separate samples of the coated support from each batch were taken for the determination of the IL loading $\lambda$. Its resulting value was established as an average of the values obtained by the different procedures for these samples, with the relative standard deviation between 1 and 2%.

From the value of $\lambda$ and the mass of the coated support charged in the column the mass of the IL in the column was determined.

**Retention Measurements.** The column installed into the chromatograph was first conditioned by gradual heating up to 105 °C under a moderate flow of nitrogen for 2 days. Afterward, the column was removed from the chromatograph and reweighed. No significant weight loss was observed. Three columns of two different lengths loaded with [EMIM][$NO_3$] ($\lambda$ being 0.11 and 0.15) were used.

The retention measurements were carried out at several temperatures, namely 318.15, 323.15, 333.15, 343.15, and 353.15 K, and nominal flow rates of 10 and 50 $cm^3$/min. At a given temperature, each experiment was replicated three times in a sequence (during 1 day) and at least two times during a longer period of time, to check the reproducibility. The precise carrier gas flow rate values were determined with an uncertainty of 0.5%, using a soap bubble flow-meter placed at the outlet of the column. The long-term stability of the flow rates maintained by a mass flow controller of the GC was periodically checked. The outlet pressure $p_0$ was equal to the atmospheric pressure which was measured using a mercury barometer with an uncertainty of 0.05 kPa. The pressure drop ($p_i - p_0$), measured by the chromatograph with an uncertainty of 0.1 kPa, varied between 7 and 44 kPa depending on the carrier gas flow rate, temperature and length of the column. The temperature of the column was regulated by the oven thermostat of the chromatograph. On the basis of the independent measurements by a calibrated platinum resistance thermometer, the absolute uncertainty in the experimental temperature was estimated to 0.2 K.

To ensure the state of infinite dilution, the volume of the sample injected into the column was chosen to be the lowest possible, that is, 0.1 $\mu$L. Parallel measurements with 0.1 $\mu$L injection of 10% solution of individual solutes in hexane were carried out for solutes miscible with hexane and with retention time sufficiently different from it. For alkanes, oct-1-ene, cycloalkanes and benzene parallel measurements with 2.5 $\mu$L injection of vapor samples were carried out. As no differences in retention were observed for all solutes studied, it can be assumed that the state of infinite dilution was achieved to a high degree of approximation for injections of 0.1 $\mu$L of these pure solutes. The resolution in retention time measurements was 0.001 min, nevertheless a realistic estimate of the uncertainty in determination of the retention time $t_R$ and the retention time of the nonretainable component (methane) $t_D$ was assumed to be 0.01 min. Absolute values of the adjusted retention times ($t_R - t_D$) varied between 0.1 and 70 min depending on solute, temperature, and column used.

After preliminary determination of the retention times of individual solutes, the retention measurements were automated and were run in sequences. Retention times of one check solute (to check sequence-to-sequence reproducibility of conditions) and five to seven other solutes were measured in the entire temperature range in each sequence.

**TABLE 1: Experimental Infinite Dilution Activity Coefficients $\gamma_1^\infty$ of Organic Solutes in [EMIM][$NO_3$], Constants *a* and *b* of Equation 6, and Standard Deviation *s* of the Fit**

| | $\gamma_1^\infty$ | | | | | | | |
|---|---|---|---|---|---|---|---|---|
| solute | 318.15 K | 323.15 K | 333.15 K | 343.15 K | 353.15 K | *a*/K | *b* | *s* |
| heptane | 464 | 433 | 418 | 390 | 384 | 589.6 | 4.266 | 0.022 |
| octane | 641 | 629 | 607 | 579 | 569 | 398.9 | 5.209 | 0.007 |
| oct-1-ene | 303 | 295 | 284 | 275 | 265 | 425.4 | 4.374 | 0.004 |
| cyclohexane | 121 | 116 | 109 | 102 | 97.2 | 694.7 | 2.606 | 0.006 |
| methylcyclohexane | 186 | 179 | 170 | 157 | 152 | 678.4 | 3.092 | 0.010 |
| ethylcyclohexane | 297 | 285 | 268 | 251 | 237 | 712.7 | 3.450 | 0.003 |
| benzene | 4.85 | 4.88 | 4.91 | 4.91 | 4.96 | −62.2 | 1.776 | 0.002 |
| toluene | 8.87 | 8.93 | 8.99 | 9.05 | 9.12 | −83.4 | 2.446 | 0.001 |
| ethylbenzene | 17.7 | 17.6 | 17.5 | 17.4 | 17.2 | 79.7 | 2.621 | 0.001 |
| *m*-xylene | 17.0 | 17.0 | 17.0 | 17.1 | 17.1 | −12.3 | 2.873 | 0.001 |
| methanol | 0.564 | 0.559 | 0.551 | 0.547 | 0.542 | 125.7 | −0.971 | 0.002 |
| ethanol | 1.14 | 1.11 | 1.08 | 1.04 | 1.02 | 350.1 | −0.975 | 0.003 |
| propan-1-ol | 1.77 | 1.73 | 1.66 | 1.60 | 1.55 | 441.7 | −0.818 | 0.003 |
| propan-2-ol | 1.97 | 1.92 | 1.84 | 1.77 | 1.72 | 431.6 | −0.682 | 0.004 |
| 2,5-dioxahexane | 3.89 | 3.99 | 4.21 | 4.42 | 4.59 | −541.9 | 3.062 | 0.003 |
| diisopropyl ether | 96.6 | 94.3 | 94.0 | 93.5 | 91.6 | 138.5 | 4.128 | 0.008 |
| *t*-butylmethyl ether | 13.1 | 13.7 | 14.5 | 15.1 | 15.5 | −619.7 | 4.530 | 0.011 |
| tetrahydrofuran | 2.87 | 2.89 | 2.91 | 2.93 | 2.94 | −86.0 | 1.325 | 0.002 |
| methyl acetate | 3.64 | 3.68 | 3.75 | 3.83 | 3.94 | −248.0 | 2.070 | 0.004 |
| ethyl acetate | 7.39 | 7.42 | 7.52 | 7.59 | 7.68 | −123.4 | 2.387 | 0.001 |
| acetone | 2.24 | 2.26 | 2.31 | 2.36 | 2.40 | −230.7 | 1.530 | 0.001 |
| butanone | 4.00 | 4.03 | 4.11 | 4.13 | 4.18 | −138.1 | 1.822 | 0.004 |
| dimethyl carbonate | 3.19 | 3.21 | 3.25 | 3.29 | 3.32 | −133.4 | 1.580 | 0.001 |
| dichloromethane | 0.632 | 0.651 | 0.691 | 0.729 | 0.769 | −628.8 | 1.517 | 0.001 |
| chloroform | 0.813 | 0.855 | 0.941 | 1.04 | 1.13 | −1065.8 | 3.141 | 0.002 |
| halothane | 1.20 | 1.29 | 1.46 | 1.65 | 1.85 | −1377.9 | 4.515 | 0.002 |
| tetrachloromethane | 6.67 | 6.82 | 7.18 | 7.51 | 7.83 | −520.0 | 3.531 | 0.002 |
| nitromethane | 0.805 | 0.814 | 0.829 | 0.846 | 0.862 | −217.2 | 0.466 | 0.001 |
| acetonitrile | 1.06 | 1.07 | 1.08 | 1.09 | 1.10 | −124.6 | 0.452 | 0.002 |
| thiophene | 1.39 | 1.41 | 1.44 | 1.47 | 1.51 | −251.6 | 1.121 | 0.001 |

**TABLE 2: Experimental Gas−Liquid Partition Coefficients $K_L$ of Organic Solutes in [EMIM][$NO_3$], Constants *a* and *b* of $\ln K_L = a/T + b$, and Standard Deviation *s* of the Fit**

| | $K_L$ | | | | | | | |
|---|---|---|---|---|---|---|---|---|
| solute | 318.15 K | 323.15 K | 333.15 K | 343.15 K | 353.15 K | *a*/K | *b* | *s* |
| heptane | 2.53 | 2.23 | 1.60 | 1.21 | 0.90 | 3353.7 | −9.595 | 0.019 |
| octane | 5.29 | 4.31 | 2.93 | 2.08 | 1.47 | 4087.7 | −11.186 | 0.006 |
| oct-1-ene | 9.25 | 7.66 | 5.28 | 3.73 | 2.72 | 3940.9 | −10.163 | 0.005 |
| cyclohexane | 4.97 | 4.36 | 3.31 | 2.59 | 2.04 | 2862.8 | −7.393 | 0.005 |
| methylcyclohexane | 6.41 | 5.52 | 4.08 | 3.16 | 2.40 | 3140.0 | −8.011 | 0.009 |
| ethylcyclohexane | 12.8 | 10.7 | 7.56 | 5.50 | 4.08 | 3679.9 | −9.018 | 0.003 |
| benzene | 125 | 103 | 73.0 | 53.1 | 39.2 | 3697.8 | −6.805 | 0.005 |
| toluene | 205 | 166 | 112 | 77.9 | 55.3 | 4200.7 | −7.885 | 0.004 |
| ethylbenzene | 276 | 220 | 145 | 97.4 | 67.7 | 4512.2 | −8.566 | 0.005 |
| *m*-xylene | 325 | 258 | 167 | 111 | 75.8 | 4673.3 | −8.908 | 0.004 |
| methanol | 716 | 587 | 401 | 280 | 201 | 4088.9 | −6.278 | 0.001 |
| ethanol | 686 | 555 | 370 | 254 | 178 | 4337.7 | −7.105 | 0.002 |
| propan-1-ol | 1094 | 867 | 556 | 367 | 249 | 4751.6 | −7.939 | 0.003 |
| propan-2-ol | 501 | 401 | 263 | 178 | 123 | 4502.5 | −7.939 | 0.002 |
| 2,5-dioxahexane | 200 | 160 | 105 | 70.5 | 49.2 | 4503.6 | −8.863 | 0.006 |
| diisopropyl ether | 4.16 | 3.59 | 2.60 | 1.94 | 1.50 | 3308.8 | −8.971 | 0.009 |
| *t*-butylmethyl ether | 19.2 | 15.6 | 10.9 | 7.92 | 5.95 | 3758.7 | −8.874 | 0.017 |
| tetrahydrofuran | 129 | 108 | 77.6 | 57.0 | 42.8 | 3540.1 | −6.272 | 0.005 |
| methyl acetate | 75.4 | 62.8 | 44.3 | 32.0 | 23.6 | 3730.5 | −7.404 | 0.002 |
| ethyl acetate | 78.7 | 64.8 | 44.7 | 31.7 | 23.0 | 3952.2 | −8.059 | 0.003 |
| acetone | 118 | 98.6 | 70.3 | 51.2 | 38.1 | 3627.3 | −6.633 | 0.003 |
| butanone | 155 | 127 | 87.4 | 62.9 | 45.8 | 3906.0 | −7.241 | 0.009 |
| dimethyl carbonate | 300 | 244 | 164 | 114 | 81.2 | 4203.9 | −7.512 | 0.005 |
| dichloromethane | 239 | 199 | 140 | 101 | 74.4 | 3752.7 | −6.320 | 0.003 |
| chloroform | 383 | 308 | 204 | 139 | 96.7 | 4424.0 | −7.958 | 0.003 |
| halothane | 178 | 142 | 92.9 | 62.1 | 42.9 | 4569.5 | −9.184 | 0.003 |
| tetrachloromethane | 78.2 | 64.3 | 44.0 | 31.1 | 22.4 | 4012.9 | −8.256 | 0.004 |
| nitromethane | 1780 | 1430 | 949 | 645 | 451 | 4409.8 | −6.379 | 0.003 |
| acetonitrile | 608 | 504 | 352 | 252 | 184 | 3830.5 | −5.632 | 0.002 |
| thiophene | 508 | 417 | 287 | 203 | 147 | 3994.8 | −6.328 | 0.003 |

## Results

Infinite dilution activity coefficients and gas−liquid partition coefficients in [EMIM][$NO_3$] were determined for a set of 30 selected solutes at 318.15, 323.15, 333.15, 343.15, and 353.15 K. Retention measurements were carried out on three columns loaded with different amounts of the IL, namely 1.194 ($\lambda$ = 0.11), 1.413 ($\lambda$ = 0.15) and 2.064 g ($\lambda$ = 0.15). The values of $\gamma_1^\infty$ and $K_L$ were calculated using eqs 1 and 2 from measured solute retention and other data specified as follows. The saturated vapor pressures $p_1^s$ and densities of pure solutes were calculated from the respective temperature dependences recommended in the database of thermodynamic properties CDATA.[18] For solutes

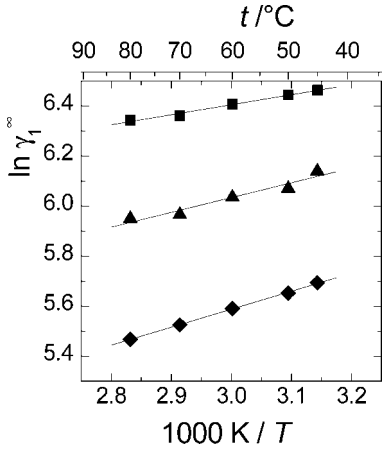


**Figure 3.** Temperature dependence of limiting activity coefficient of some solutes with strongly endothermic dissolution in [EMIM][NO$_3$]: ■, octane; ▲, heptane; ◆, ethylcyclohexane.

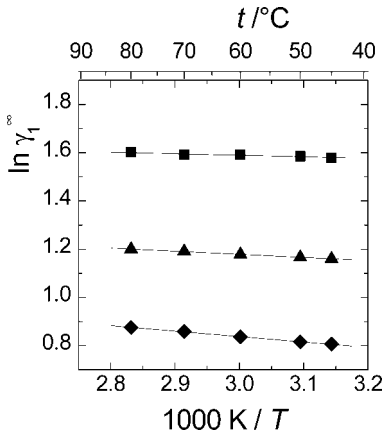


**Figure 4.** Temperature dependence of limiting activity coefficient of some solutes with nearly athermal dissolution in [EMIM][NO$_3$]: ■, benzene; ▲, dimethyl carbonate; ◆, acetone.

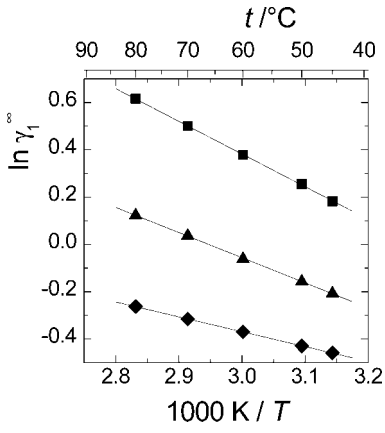


**Figure 5.** Temperature dependence of limiting activity coefficient of some solutes with strongly exothermic dissolution in [EMIM][NO$_3$]: ■, halothane; ▲, chloroform; ◆, dichloromethane.

not listed in CDATA temperature dependences recommended by Steele at al.[19] were used. The virial coefficient values $B_{11}$ and $B_{12}$ were estimated by the Hayden−O'Connell method.[20] Parameters needed for the estimation of $B_{11}$ and $B_{12}$ were taken from CDATA and Prausnitz et al.[21] The values of $p_1^s$, $v_1^L$, $B_{11}$ and $B_{12}$ used are tabulated in Supporting Information. Partial molar volumes $\bar{v}_1^\infty$ were approximated by the molar volumes of pure liquid solutes $v_1^L$. The liquid density of [EMIM][NO$_3$] has not been reported in the literature. The $\rho_3$ data, needed to calculate $K_L$ values, were therefore estimated from those available for other two 1-alkyl-3-methylimdazolium nitrates (alkyl = butyl, hexyl),[22] considering that the density of 1-alkyl-3-methylimidazolium ILs decreases approximately linearly with the increasing alkyl chain length. In the temperature range of our GLC measurements, $\rho_3$ of [EMIM][NO$_3$] was thus obtained from $\rho_3/(g\cdot cm^{-3}) = 1.1661-6.910\cdot10^{-4}$ ($T$/K).

**TABLE 3: Limiting Partial Molar Excess Enthalpies $\bar{H}_1^{E,\infty}$, Entropies $T_{ref}\bar{S}_1^{E,\infty}$ and Gibbs energies $\bar{G}_1^{E,\infty}$ of Organic Solutes in [EMIM][NO$_3$] at a Reference Temperature $T_{ref}$ = 323.15 K**

| solute | $\bar{H}_1^{E,\infty}$ (kJ·mol$^{-1}$) | $T_{ref}\bar{S}_1^{E,\infty}$ (kJ·mol$^{-1}$) | $\bar{G}_1^{E,\infty}$ (kJ·mol$^{-1}$) |
|---|---|---|---|
| heptane | 4.9 | −11.5 | 16.4 |
| octane | 3.3 | −14.0 | 17.3 |
| oct-1-ene | 3.5 | −11.8 | 15.3 |
| cyclohexane | 5.8 | −7.0 | 12.8 |
| methylcyclohexane | 5.6 | −8.3 | 13.9 |
| ethylcyclohexane | 5.9 | −9.3 | 15.2 |
| benzene | −0.5 | −4.7 | 4.3 |
| toluene | −0.7 | −6.6 | 5.9 |
| ethylbenzene | 0.7 | −7.0 | 7.7 |
| *m*-xylene | −0.1 | −7.7 | 7.6 |
| methanol | 1.0 | 2.6 | −1.6 |
| ethanol | 2.9 | 2.6 | 0.3 |
| propan-1-ol | 3.7 | 2.2 | 1.5 |
| propan-2-ol | 3.6 | 1.8 | 1.8 |
| 2,5-dioxahexane | −4.5 | −8.2 | 3.7 |
| diisopropyl ether | 1.2 | −11.1 | 12.2 |
| *t*-butylmethyl ether | −4.5 | −11.5 | 7.0 |
| tetrahydrofuran | −0.7 | −3.5 | 2.8 |
| methyl acetate | −2.1 | −5.6 | 3.5 |
| ethyl acetate | −1.0 | −6.4 | 5.4 |
| acetone | −1.9 | −4.1 | 2.2 |
| butanone | −1.1 | −4.9 | 3.7 |
| dimethyl carbonate | −1.1 | −4.2 | 3.1 |
| dichloromethane | −5.2 | −4.1 | −1.2 |
| chloroform | −8.9 | −8.4 | −0.4 |
| halothane | −11.5 | −12.1 | 0.7 |
| tetrachloromethane | −4.3 | −9.5 | 5.2 |
| nitromethane | −1.8 | −1.3 | −0.6 |
| acetonitrile | −1.0 | −1.2 | 0.2 |
| thiophene | −2.1 | −3.0 | 0.9 |

Figure 1 demonstrates on three solutes, that the correspondence of $\gamma_1^\infty$ values obtained on columns loaded with different amounts of [EMIM][NO$_3$] was very good, the values being within ±1.5% from the mean for the majority of the solutes. However, a few solutes with very weak retention (alkanes, cycloalkanes, diisopropyl ether) showed larger differences

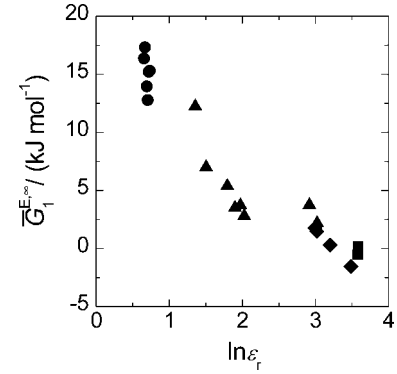


**Figure 6.** Correlation of limiting dissolution Gibbs energy $\bar{G}_1^{E,\infty}$ with dielectric constant $\varepsilon_r$ for various solutes in [EMIM][NO$_3$] at 323.15 K: ●, aliphatic hydrocarbons; ▲, ethers, esters, ketones; ◆, alcohols; ■, nitrogen-containing.

**TABLE 4: LFER System Constants for [EMIM][NO$_3$] at 323.15 K**

| | system constants[a] | | | | | | statistics[b] | | | |
|---|---|---|---|---|---|---|---|---|---|---|
| set of solutes | *e* | *s* | *a* | *b* | *l* | *c* | $r^2$ | SD | *F* | *n* |
| complete | 0.63 (0.24) | 2.66 (0.23) | 3.96 (0.44) | 0 | 0.27 (0.10) | −0.36 (0.32) | 0.953 | 0.187 | 126 | 30 |
| outliers excluded[c] | 0.75 (0.16) | 2.76 (0.16) | 4.32 (0.29) | 0 | 0.35 (0.07) | −0.71 (0.22) | 0.982 | 0.121 | 294 | 27 |

[a] Values in parentheses are standard uncertainties of the parameters. [b] $r^2$, coefficient of determination; SD, standard deviation of fit; *F*, Fischer's statistics; *n*, number of solutes. [c] Outliers: halothane, dimethyl carbonate, MTBE.

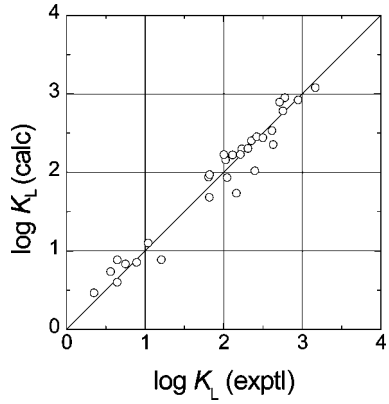


**Figure 7.** Calculated vs experimental logarithmic gas−liquid partition coefficients log $K_L$ for 30 solutes in [EMIM][NO$_3$] at 323.15 K using the LFER solvation model.

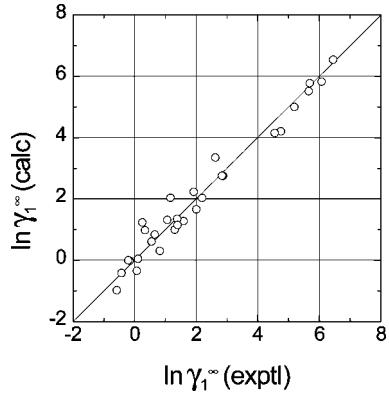


**Figure 8.** Calculated vs experimental logarithmic infinite dilution activity coefficients ln $\gamma_1^\infty$ for 30 solutes in [EMIM][NO$_3$] at 323.15 K using the LFER solvation model.

between the results from the three columns, as illustrated in Figure 2. The enhanced dispersion of results follows here from the enhanced relative uncertainty of the retention time determination and is fully accounted for by the estimated combined standard uncertainty. Although the dispersion appears to be somewhat systematic, the trends observed are incompatible with interfacial adsorption effects. If the adsorption effects were significant, the $\gamma_1^\infty$ values measured on the column with lower IL loading (1.194 g IL, $\lambda = 0.11$) should have been systematically lower than those obtained on the columns with higher IL loadings ($\lambda = 0.15$) and this disparity should have diminished with increasing temperature. Since the opposite was observed, the effect of adsorption on the gas−liquid interphase was considered to be negligible.

The average $\gamma_1^\infty$ and $K_L$ values obtained from measurements on the three columns are listed in Table 1 and 2, respectively. Weighted averaging rather than the simple one was used in some cases of weakly retained solutes where the relative uncertainty of retention time determined on the three columns varied considerably. Given in the tables are also parameters of respective equations fitting the temperature dependence of the data and the standard deviations of fits.

As estimated on the basis of the error propagation law, the combined standard uncertainty of the resulting $\gamma_1^\infty$ and $K_L$ values in Tables 1 and 2 lies for most of the solutes between 2 and 3%. Higher uncertainty should be however allowed for solutes exhibiting very short retention times, namely, from 3 to 5% for octane and cycloalkanes and from 5 to 10% for heptane and diisopropyl ether.

## Discussion

**Thermodynamic Properties of Solution and Molecular Interactions.** Figures 3−5 illustrate for selected solutes various $\gamma_1^\infty$ temperature dependences that correspond to widely different thermal effects for the dissolution of these solutes in [EMIM][NO$_3$]. Table 3 lists the limiting partial molar excess Gibbs energies $\bar{G}_1^{E,\infty} = RT \ln \gamma_1^\infty$ of all the studied solutes in [EMIM][NO$_3$] at a reference temperature 323.15 K together with their enthalpy ($\bar{H}_1^{E,\infty}$) and entropy ($T_{ref}\bar{S}_1^{E,\infty}$) contributions, as calculated from the temperature dependence of limiting activity coefficient. The standard uncertainties of the $\bar{H}_1^{E,\infty}$ and $T_{ref}\bar{S}_1^{E,\infty}$ values, estimated taking into account the uncertainties of our $\gamma_1^\infty$ values and the stability of their fits according to eq 6, are from 0.7 to 1.0 kJ/mol for the majority of the solutes. For weakly retained solutes (aliphatic hydrocarbons, diisopropyl ether), one should allow for uncertainties from 1 to 3 kJ/mol.

As seen from Table 3, the solution behavior of aliphatic hydrocarbons differs distinctly from that of other solutes. Since the IL studied in this work is a highly cohesive solvent medium of substantial polarity, the considerably larger $\bar{G}_1^{E,\infty}$ values found for aliphatic hydrocarbons indicate that the solute-IL interactions are for nonpolar aliphatic hydrocarbon solutes much weaker than for polar solutes or solutes with polarizable/delocalized electrons. Obviously, the higher the cohesive energy density of the solvent, the more energy has to be spent for breaking the solvent−solvent interactions during the solution process. In case of aliphatic hydrocarbons this energy penalty is not compensated by formation of sufficiently strong solute−solvent interactions, which leads to poor miscibility of the aliphatics with [EMIM][NO$_3$]. In the series of hydrocarbons, the solution nonideality is seen to decrease in the following sequence: alkanes > alkenes (1-octene) > cycloalkanes > aromatics. The same pattern of hydrocarbon solution behavior has been observed also for the majority of other ILs, but it is especially noticeable in case of ILs composed of small ions lacking any large nonpolar substituents. In such ILs the charge density of ions is high, which causes them to be more selective. The rationale for the sequence given above seems to be also clear: while the introduction of a double bond brings polarizable electrons favorably interacting with the positive charge of the IL cation and the cyclization makes the solute molecule more compact saving thus even more energy upon the cavity formation in the highly cohesive IL, the introduction of the aromatic $\pi$-electron system causes the hydrocarbon solute to interact strongly with the IL ionic charge and yields the most favorable energetic effect.

**TABLE 5: Comparison of LFER System Constants for Several Liquids at 354 K[a]**

| solvents | system constants[b] | | | | | | statistics[c] | | | |
|---|---|---|---|---|---|---|---|---|---|---|
| | *e* | *s* | *a* | *b* | *l* | *c* | $r^2$ | SD | *F* | *n* |
| molecular liquids | | | | | | | | | | |
| squalane | 0.07 (0.03) | 0 | 0 | 0 | 0.73 (0.01) | −0.19 (0.02) | 0.998 | 0.025 | 7638 | 22 |
| Carbowax 20 M | 0.27 (0.08) | 1.52 (0.07) | 2.16 (0.13) | 0 | 0.53 (0.02) | −0.42 (0.10) | 0.988 | 0.053 | 311 | 21 |
| 1,2,3-tris(2-cyanoethoxy)propane | 0.29 (0.10) | 2.17 (0.10) | 1.99 (0.18) | 0.28 (0.11) | 0.36 (0.02) | −0.48 (0.12) | 0.986 | 0.062 | 213 | 22 |
| ionic liquids | | | | | | | | | | |
| butylammonium thiocyanate | 0.14 (0.09) | 1.65 (0.09) | 2.76 (0.16) | 1.32 (0.11) | 0.45 (0.02) | −0.75 (0.10) | 0.990 | 0.058 | 326 | 23 |
| ethylammonium nitrate | 0.47 (0.16) | 2.21 (0.16) | 3.38 (0.28) | 1.03 (0.17) | 0.21 (0.04) | −0.87 (0.20) | 0.988 | 0.089 | 175 | 17 |
| 1-ethyl-3-methylimidazolium nitrate | 0.83 (0.14) | 2.50 (0.14) | 3.78 (0.26) | 0 | 0.24 (0.06) | −0.78 (0.20) | 0.983 | 0.109 | 327 | 27 |

[a] Results for [EMIM][$NO_3$] are from this work, for all other solvents from reference 12. [b] Values in parentheses are standard uncertainties of the parameters. [c] $r^2$, coefficient of determination; SD, standard deviation of fit; *F*, Fischer's statistics; *n*, number of solutes.

**TABLE 6: Contribution of Solvent Cavity Formation and Solute−Solvent Dispersion Interactions to log $K_L$ of Octane at 354 K**

| solvent | $c + lL$ |
|---|---|
| squalane | 2.49 |
| Carbowax 20 M | 1.53 |
| butylammonium thiocyanate | 0.90 |
| 1,2,3- tris(2-cyanoethoxy)propane | 0.84 |
| 1-ethyl-3-methylimidazolium nitrate | 0.10 |
| ethylammonium nitrate | −0.10 |

Looking now at other than hydrocarbon solutes, one can see that a similar level of nonideality as for cycloalkanes is also encountered for diisopropyl ether. The finding is not surprising if one realizes that the oxygen atom in its relatively bulky molecule is shielded by alkyl moieties and hence the oxygen is not easily accessible for interactions with the ILs. 2,5-Dioxahexane, esters, ketones, and tetrachloromethane show weaker positive deviations from Raoult's law which are comparable with those for benzene. Ion−dipole and/or ion-induced dipole interactions are probably the main cause of this weakening of nonideality. Low values of $\gamma_1^\infty$, corresponding often to negative deviations from ideality, were obtained for alcohols, dichloromethane, chloroform, halothane, thiophene, and polar nitrogen containing compounds of small molecular size (nitromethane, acetonitrile). While for dichloromethane, chloroform and halothane (nonself-associated strong proton donors) the thermodynamically favorable dissolution is essentially due to their hydrogen bonding complex formation with the IL solvent, for other solutes the prevailing interaction mechanism is not clear. Nevertheless, it is interesting to note that the solute polarity, as measured by the dielectric constant $\varepsilon_r$, is an essential factor and, provided solutes specifically interacting with the ILs studied are excluded, also a possible solute descriptor correlating with $\bar{G}_1^{E,\infty}$ (see Figure 6).

In a given group of solutes, the $\gamma_1^\infty$ values increase with increasing number of carbon atoms, which is a general behavior observed also for other IL solvents. To a great extent this trend stems from the energetic weakness of solute−solvent interaction but at least partly it may be also due to the combinatorial entropy arising from different sizes of solvent and solute molecules; when the size of the solute molecule increases and approaches that of the IL solvent, the favorable combinatorial entropy effect diminishes.

Large positive $\bar{G}_1^{E,\infty}$ values encountered for aliphatic hydrocarbons and corresponding to their low solubilities in [EMIM]-[$NO_3$], are seen to be mainly of the entropic origin. Also for most of the remaining solutes the thermal effect of solution is rather small, being effectively nil for aromatics. Large negative $\bar{H}_1^{E,\infty}$ values of strong proton donors (halothane, chloroform, and dichloromethane), caused by formation of strong hydrogen bonds with the IL, are more or less counterbalanced by large negative solution entropies and give rise to small $\gamma_1^\infty$ values of these solutes. This suggests that [EMIM][$NO_3$] is an efficient proton acceptor, the source of its hydrogen bond basicity being most probably both the multiple lone electron pairs of its nitrate anion and the $\pi$-electron system of its imidazolium cation. For all solutes but alcohols, the solution in [EMIM][$NO_3$] is associated with significant entropy losses. Positive values of $\bar{S}_1^{E,\infty}$ for alcohols result from breaking their hydrogen bond structures during the solution process. The entropy contribution to $\bar{G}_1^{E,\infty}$ is important for all solutes, but it is entirely predominant in case of aromatics forming around 90% of their $\bar{G}_1^{E,\infty}$. This may suggest that aromatics as well as other solute molecules arrange in the IL structure, following highly orientational character of involved intermolecular forces.

**LFER Solvation Model Correlation and Molecular Interactions.** There have been numerous reports of methods for correlation and prediction of gas−liquid partitioning. Among them, the simple linear free energy relationship (LFER) solvation model of Abraham[23,24] has been proved to perform well for large sets of solutes in a wide variety of solvent media, including ILs.[12,25−28] In particular, the LFER model has been shown[12,26,29−32] to provide a powerful tool for analyzing the contributions of individual intermolecular interactions to the gas−liquid partitioning process and hence it was applied to this end also in this work. The LFER model considers contributions for solvent cavity formation and solute−solvent interactions identified as dispersion, electron-lone pair, dipole-type, and hydrogen bonding. The LFER equation was used here in the form

$$\log K_L = c + eE + sS + aA + bB + lL \qquad (7)$$

where the capital letters (*E*, *S*, *A*, *B*, *L*) are the solute descriptors and the lower case letters (*e*, *s*, *a*, *b*, *l*) are the system constants representing respective contributions from the solvent. The *c* term is the model constant. The solute descriptors are *E* the excess molar refraction (solute tendency to interact through lone electron pairs), *S* the solute dipolarity/polarizibility, *A* the solute effective hydrogen bond acidity, *B* the solute hydrogen bond basicity, *L* the logarithm of the gas−hexadecane partition coefficient (298 K). The *L* descriptor involves the contributions of solute to the solvent cavity formation and the solute−solvent dispersion interactions. The Abraham's solute descriptors are available for a large number of compounds,[23,28] including those studied in this work for which we list them in Supporting Information. The system constants can be calculated from experimental $K_L$ values for a set of solutes using standard procedures of multiple regression analysis. Provided the solute

**TABLE 7: Selectivities $S_{12}^{\infty}$ of Some Ionic Liquids and Molecular Solvents for Two Aliphatic/Aromatic Hydrocarbon Separation Pairs at 323.15 K**

| | $S_{12}^{\infty}$ | | |
|---|---|---|---|
| solvent | cyclohexane (1)−benzene (2) | heptane (1)−toluene (2) | ref |
| 1,2-dimethyl-3-propylimidazolium tetrafluoroborate | 27.2 | 59.4 | 33 |
| acryloyloxypropyl-*N*-methylimidazolium bromide | 25.6 | 13.9 | 34 |
| 1,3-dimethylimidazolium methoxyethylsulphate | 24.7 | 37.6 | 11 |
| 1-ethyl-3-methylimidazolium nitrate | 23.9 | 49.5 | this work |
| 1-ethyl-3-methylimidazolium tetrafluoroborate | 18.5 | 41.6 | 35 |
| 1,3-dimethylimidazolium methylsulfate | 16.2 | 15.2 | 11 |
| 1,3-dimethylimidazolium bis(trifluoromethylsulfonyl)imide | 14.2 | 26.7 | 36 |
| 1-ethyl-3-methylimidazolium trifluoroacetate | 11.9 | 24.0 | 37 |
| 1-ethyl-3-methylimidazolium bis(trifluoromethylsulfonyl)imide | 11.2 | 20.5 | 36 |
| 1-propenyl-3-methylimidazolium bromide | 4.4 | 8.0 | 38 |
| sulfolane | 11.0 | 19.5 | 39[a] |
| dimethylsulfoxide (DMSO) | 8.8 | 15.7 | 39[a] |
| N-methyl-2-pyrrolidinone (NMP) | 6.5 | 9.5 | 39[a] |
| N,N-dimethylformamide (DMF) | 6.4 | 9.4 | 39[a] |
| diethylene glycol (DEG) | 6.2 | 13.0 | 39[a] |

[a] Selectivity values given are based on a comprehensive critical compilation of available $\gamma^{\infty}$ literature data and their temperature dependence fit.

**TABLE 8: Selectivities $S_{12}^{\infty}$ of Some Ionic Liquids and Molecular Solvents for Three Thiophene/Hydrocarbon Separation Pairs at 323.15 K**

| | $S_{12}^{\infty}$ | | | |
|---|---|---|---|---|
| solvent | octane (1) −thiophene (2) | cyclohexane (1) −thiophene (2) | benzene (1) −thiophene (2) | ref |
| 1-ethyl-3-methylimidazolium nitrate | 450 | 82.3 | 3.46 | this work |
| acryloyloxypropyl-N-methylimidazolium bromide | 75.6 | 52.7 | 2.06 | 34 |
| 1-butyl-3-methylimidazolium hexafluorophosphate | 66.4 | 14.7 | 1.33 | 13 |
| 1-butyl-3-methylimidazolium trifluoromethanesulfonate | 54.8 | 14.5 | 1.37 | 40 |
| 1-propenyl-3-methylimidazolium bromide | 42.6 | 10.6 | 2.43 | 38 |
| 1-hexadecyl-3-methylimidazolium tetrafluoroborate | 3.28 | 2.04 | 0.95 | 41 |
| sulfolane | 61.9 | 16.3 | 1.48 | 39[a] |
| N-methyl-2-pyrrolidinone (NMP) | 20.1 | 9.03 | 1.38 | 39[a] |

[a] Selectivity values given are based on a comprehensive critical compilation of available $\gamma^{\infty}$ literature data and their temperature dependence fit.

set is sufficiently representative from the chemical and statistical point of view, the calculated system constants are not mere correlation parameters but have physical significance, their magnitudes indicating the relative importance of individual intermolecular interactions for a given solvent (ionic liquid).

The system constants calculated for [EMIM][$NO_3$] at 323.15 K are listed together with some corresponding statistical characteristics of the fit in Table 4. Values of the coefficient determination, standard deviation of fit, Fischer *F*-statistics, and the standard deviations of the individual system constants indicate consistently that the fitting results are statistically sound. Note that parameter *b* was firmly set to zero since our preliminary calculations showed its value to be statistically insignificant. The very good performance of the LFER solvation model is graphically illustrated in Figures 7 and 8. Furthermore, as seen from Table 4 the values of system parameters are virtually unaffected when some correlation outliers are excluded. This fact means that the correlation is sufficiently robust and can be considered as truly representative.

Considering the magnitudes of its system constants, [EMIM][$NO_3$] can be classified as an extremely cohesive solvent which possesses a high capacity for participating in lone electron pair interactions, dipole-type interactions, and hydrogen-bonding-type interactions with solutes of complementary capabilities. To put this into the perspective with other solvents of varying polarity, values of system constants for two other ILs and three molecular solvents as obtained by Poole[12] are compared in Table 5 with those for [EMIM][$NO_3$] at 354 K (Poole's experimental temperature). The solvent cohesion as an opposing factor to the solute solvation can be relatively assessed by the compound term ($c + lL$).[26] For the solvents considered and octane as a probe solute, this term is given in Table 6. The solvents in Table 6 are listed in the order of the decreasing ($c + lL$) term, that is, in the order of their increasing cohesion: the weakest cohesion observed for the nonpolar squalane is seen to gradually increase with the solvent polarity and ionization, becoming the strongest for nitrate ILs between whose relatively small ions strong Coulombic forces operate. The picture of [EMIM][$NO_3$] as an extremely cohesive liquid is consistent with the recent determination of its vaporization enthalpy (168.4 kJ·mol$^{-1}$ at 298 K)[15] which belongs to the highest among ILs examined so far. As indicated by the values of system constants in Table 5, [EMIM][$NO_3$] turns out to be extreme also in its selectivity for specific interactions. The tendency to interact with solutes through lone electron pairs (system constant *e*) is for [EMIM][$NO_3$] substantially higher than for any other solvent considered. Taking into account the difference from ethylammonium nitrate, it is apparent that the $\pi$-electrons in the ring of imidazolium cation contribute considerably to this tendency. The dipolarity/polarizability (system constant *s*) of [EMIM][$NO_3$] is also the highest among the solvents considered in Table 6. Nevertheless, the relative difference from 1,2,3-tris(2-cyanoethoxy)propane, one of the most polar GC stationary phases, is not too big and hence the capabilities of [EMIM][$NO_3$] and strongly polar

molecular liquids to participate in dipole/induced dipole-type interactions appear to be similar. The proton accepting ability of [EMIM][$NO_3$] (system constant $a$) surpasses considerably that of Carbowax 20M, a typical GC stationary phase of high hydrogen-bond basicity, and is also higher than those for other ILs. However, in contrast to the alkylammonium ILs which are also strong hydrogen bond acids, [EMIM][$NO_3$] has no such capability (system constant $b = 0$).

**Separation Selectivity of [EMIM][$NO_3$].** An important prospective application of ILs is their utilization in separation processes. In this respect, the separation selectivity of [EMIM]-[$NO_3$] is discussed in this section and compared with characteristics of some other ILs and molecular solvents for the separation of aromatic hydrocarbons and thiophene from aliphatic hydrocarbons. Selectivities $S_{12}^{\infty} = \gamma_1^{\infty}/\gamma_2^{\infty}$ at 323.15 K, as derived from the limiting activity coefficient values of the components to be separated, were determined here for the model pairs cyclohexane (1)−benzene (2) and heptane (1)−toluene (2) (Table 7) and octane (1)−thiophene (2), cyclohexane (1)−thiophene (2), and benzene (1)−thiophene (2) (Table 8).

As seen in Table 7, [EMIM][$NO_3$] turns out to be a potentially very good solvent for separation of aromatic from saturated hydrocarbons: its selectivity $S_{12}^{\infty}$ for these mixtures belongs to the highest among all the ILs in which $\gamma^{\infty}$ values for these solutes have been determined and considerably surpasses those exhibited by molecular solvents. It should be noted that the capacity, $\kappa_1^{\infty} = 1/\gamma_2^{\infty}$, of [EMIM][$NO_3$] for the aromatics to be extracted (benzene and toluene) is however less favorable (0.21 and 0.11, respectively). Table 8 reveals that for the separation of thiophene from aliphatic hydrocarbons [EMIM]-[$NO_3$] gives an extremely high selectivity, superior to those for other solvents studied so far. For the separation of thiophene from the aromatics, which presents generally a very difficult problem, [EMIM][$NO_3$] brings also some separation enhancement (cf. $S_{12}^{\infty}$ values for benzene (1)−thiophene (2)). Hence, [EMIM][$NO_3$] could be potentially used as an extractant for liquid fuel desulfurization, an urgent technological task which has been recently addressed by a number of researchers.[40,42−45]

## Conclusions

In this work, we have examined interactions of various types of organic solutes with the ionic liquid [EMIM][$NO_3$] through methodical GLC retention measurements. Infinite dilution activity coefficients and gas−liquid partition coefficients of 30 hydrocarbons, alcohols, ketones, ethers, esters, haloalkanes, and nitrogen- or sulfur-containing VOCs in [EMIM][$NO_3$] have been determined over a range of temperatures, which allowed derivation of respective enthalpic and entropic contributions. The finding that the entropic term plays in all cases an essential role and prevails over the enthalpic one for the majority of solutes suggests a highly orientational character of involved intermolecular forces and a structure arrangement of the IL.

Analysis of the obtained thermodynamic properties and their interpretation in terms of the LFER solvation model disclose [EMIM][$NO_3$] as an extremely cohesive solvent medium, capable of interacting strongly through lone electron pairs, dipolarity/polarizibility, and hydrogen bonding with solutes of complementary capabilities. In the hydrogen bonding, [EMIM]-[$NO_3$] has been found to act always as an proton acceptor lacking the proton donating capability.

Because of its capacity for specific interations, [EMIM][$NO_3$] as a solvent medium offers a high separation selectivity and could be thus of interest for use in solvent-aided separation processes or gas−liquid chromatography. Its superior selectivity has been convincingly demonstrated in this work for the separation of aromatic hydrocarbons and thiophene from aliphatics.

**Acknowledgment.** This work was supported from Ministry of Education of the Czech Republic (grant no. MSM 604 613 7307).

**Supporting Information Available:** Table 1S. Values of pure solute vapor pressure $p_1^s$, liquid molar volume $v_1^L$, and second virial coefficients $B_{11}$ and $B_{12}$ used in the calculation of infinite dilution activity coefficients $\gamma_1^{\infty}$ and gas−liquid partition coefficients $K_L$. Table 2S. Abraham's solute descriptors ($E$, $S$, $A$, $B$, $L$) used in the LFER solvation model correlation. This material is available free of charge via the Internet at http://pubs.acs.org.

## References and Notes

(1) Wasserscheid, P.; Welton, T. *Ionic Liquids in Synthesis*; Willey-VCH: Weinheim, Germany, 2002.
(2) Wasserscheid, P.; Keim, W. *Angew. Chem., Int. Ed.* **2000**, *39*, 3772–3789.
(3) Rogers, R. D.; Seddon, K. R. *Ionic Liquids: Industrial Applications to Green Chemistry*; ACS Symposium Series 818; American Chemical Society: Washington, DC, 2002.
(4) Rogers, R. D.; Seddon, K. R. *Ionic Liquids as Green Solvents: Progress and Prospects*; ACS Symposium Series 856; American Chemical Society: Washington, DC, 2003.
(5) Rogers, R. D.; Seddon, K. R. *Ionic Liquids IIIA: Properties and Structure*; ACS Symposium Series 901; American Chemical Society: Washington, DC, 2005.
(6) Rogers, R. D.; Seddon, K. R. *Ionic Liquids IIIB. Fundamentals, Progress, Challenges, and Opportunities. Transformations and Processes;* ACS Symposium Series 915; American Chemical Society: Washington, DC, 2005.
(7) Brennecke, J. F.; Rogers, R. D.; Seddon, K. R. *Ionic Liquids IV. Not Just Solvents Anymore;* ACS Symposium Series 975; American Chemical Society: Washington, DC, 2007.
(8) Arancibia, E. L.; Castells, R. C.; Nardillo, A. M. *J. Chromatogr.* **1987**, *398*, 21–29.
(9) Heintz, A.; Kulikov, D. V.; Verevkin, S. P. *J. Chem. Eng. Data* **2001**, *46*, 1526–1529.
(10) Letcher, T. M.; Soko, B.; Ramjugernath, D.; Deenadayalu, N.; Nevines, A.; Naicker, P. K. *J. Chem. Eng. Data* **2003**, *48*, 708–711.
(11) Kato, R.; Gmehling, J. *Fluid Phase Equilib.* **2004**, *226*, 37–44.
(12) Poole, C. F. *Journal of Chromatogr., A* **2004**, *1037*, 49–82.
(13) Mutelet, F.; Butet, V.; Jaubert, J.-N. *Ind. Eng. Chem. Res.* **2005**, *44*, 4120–4127.
(14) Dohnal, V. Measurement of Limiting Activity Coefficients Using Analytical Tools. In *Measurement of the Thermodynamic Properties of Multiple Phases*; Weir, R. D., de Loos, T. W., Eds.; Elsevier: Amsterdam, 2005; pp 359−381.
(15) Emel'yanenko, V. N.; Verevkin, S. P.; Heintz, A.; Schick, C. *J. Phys. Chem. B* **2008**, *112*, 8095–8098.
(16) Conder, J. R.; Young, C. L. *Physicochemical Measurements by Gas Chromatography*; Wiley: New York, 1979.
(17) Víška, J.; Kiss, F. *J. Chromatogr.* **1974**, *91*, 333–345.
(18) Department of Physical Chemistry, Institute of Chemical Technology. *CDATA: Database of Thermodynamic and Transport Properties for Chemistry and Engineering;* FIZ Chemie GmbH: Berlin, Prague, 1991.
(19) Steele, W. V.; Chirico, R. D.; Knipmeyer, S. E.; Nguyen, A.; Smith, N. K. *J. Chem. Eng. Data* **1996**, *41*, 1285–1302.
(20) Hayden, J. G.; O'Connell, J. P. *Ind. Eng. Chem. Process Des. Dev.* **1975**, *14*, 209–216.
(21) Prausnitz, J. M.; Anderson, T. F.; Grens, E. A.; Eckert, C. A.; Hsieh, R.; O'Connell, J. P. *Computer Calculations for Multicomponent Vapor−Liquid and Liquid−Liquid Equilibrium,* 1st ed; Prentice-Hall: Englewodd Cliffs, NJ, 1980.
(22) Seddon, K. R.; Stark, A.; Torriano, G. Viscosity and Density of 1-Alkyl-3-methylimidazolium Ionic Liquids. In *Clean Solvents: Alternative Media for Chemical Reactions and Processing;* ACS Symposium Series 819; Abraham, M. A., Moens, L., Eds.; American Chemical Society: Washington, DC, 2002; pp 34−49.
(23) Abraham, M. H. *Chem. Soc. Rev.* **1993**, *22*, 73–83.
(24) Abraham, M. H.; Ibrahim, A. M.; Zissimos, J. *J. Chromatogr. A* **2004**, *1037*, 29–47.
(25) Abraham, M. H.; Andonian-Haftvan, J.; Whiting, G. S.; Leo, A. *J. Chem. Soc. Perkin Trans. 2* **1994**, 1777–1791.

(26) Poole, S. K.; Poole, C. F. *J. Chromatogr. A* **1995**, *697*, 415–427.
(27) Abraham, M. H.; Le, J.; Acree, W. E. *Collect. Czech. Chem. Commun.* **1999**, *64*, 1748–1760.
(28) Abraham, M. H.; Ibrahim, A. M.; Acree, W. E. *Fluid Phase Equilib.* **2007**, *251*, 93–109.
(29) Poole, C. F.; Poole, S. K. *J. Chromatogr. A* **2002**, *965*, 263–299.
(30) Acree, W. E.; Abraham, M. H. *J. Chem. Technol. Biotechnol.* **2006**, *81*, 1441–1446.
(31) Abraham, M. H.; Acree, W. E. *Green Chem.* **2006**, *8*, 906–915.
(32) Sprunger, L. M.; Proctor, A.; Acree, W. E.; Abraham, M. H. *Fluid Phase Equilib.* **2008**, *265*, 104–111.
(33) Wang, M. H.; Wu, J. S.; Wang, L. S.; Li, M. Y. *J. Chem. Eng. Data* **2007**, *52*, 1488–1491.
(34) Mutelet, F.; Jaubert, J.-N.; Rogalski, M.; Harmand, J.; Sindt, M.; Mieloszynski, J.-L. *J. Phys. Chem. B* **2008**, *112*, 3773–3785.
(35) Foco, G. M.; Bottini, S. B.; Quezada, N.; de la Fuente, J. C.; Peters, C. J. *J. Chem. Eng. Data* **2006**, *51*, 1088–1091.
(36) Krummen, M.; Wasserscheid, P.; Gmehling, J. *J. Chem. Eng. Data* **2002**, *47*, 1411–1417.
(37) Domanska, U.; Marciniak, A. *J. Phys. Chem. B* **2007**, *111*, 11984–11988.
(38) Mutelet, F.; Jaubert, J.-N.; Rogalski, M.; Boukherissa, M.; Dicko, A. *J. Chem. Eng. Data* **2006**, *51*, 1274–1279.
(39) *PLACID−Prague Limiting Activity Coefficient Inquiry Database;* Department of Physical Chemistry, Institute of Chemical Technology: Prague, 1999.
(40) Domanska, U.; Marciniak, A. *J. Phys. Chem. B* **2008**, *112*, 11100–11105.
(41) Mutelet, F.; Jaubert, J.-N. *J. Chem. Thermodyn.* **2007**, *39*, 1144–1150.
(42) Esser, J.; Wasserscheid, P.; Jess, A. *Green Chem.* **2004**, *6*, 316–322.
(43) Zhao, D.; Wang, J.; Zhou, E. *Green Chem.* **2007**, *9*, 1219–1222.
(44) Alonso, L.; Arce, A.; Francisco, M.; Rodriguez, O.; Soto, A. *AIChE J.* **2007**, *53*, 3108–3115.
(45) Alonso, L.; Arce, A.; Francisco, M.; Soto, A. *Fluid Phase Equilib.* **2008**, *263*, 176–181.

JP811041K